

## Photoactive Device by Electrochemical Processing of Silicon

H.J. Lewerenz, M. Aggour, T. Stempel-Pereira, M. Lublow, J. Grzanna and K. Skorupska

Division of Solar Energy

Hahn-Meitner-Institut Berlin GmbH, Glienicke Str. 100, D-14109 Berlin, Germany

The (photo)electrochemistry of silicon, although investigated for decades [1,2] knows still various aspects that remain unresolved. Among them is the rather obscure anodic dark current transient, first observed by Matsumura and Morrison [3] that has later been used to prepare electrochemically H-terminated (111) surfaces of exceptional chemical and electronic quality [4-6]. The nature of the charge injecting species, responsible for the dark current, has not yet been identified. In this context, it is also surprising that the dark current voltage characteristic of highly doped  $n^+$ -Si in fluoride containing electrolyte resembles closely that of low doped illuminated n-Si [7]. It appears that the behaviour of Si electrodes in HF and  $\text{NH}_4\text{F}$  solutions that predominantly etch silicon oxide has not yet been fully comprehended. Recently, we obtained photocorrosion which shows fractal structures in concentrated ammonium fluoride solutions [8].

Another intriguing aspect is the oscillatory behaviour of Si electrodes at higher anodic potentials ( $V > 4\text{V}$ ) in HF containing electrolytes. Regular current (and voltage) oscillations are observed for illuminated n-Si and in the dark for p-Si and  $n^+$ -Si [7,9]. As one origin of this behaviour, the existence of micro- or nanopores has been postulated [10] and indeed been found [11]. The pore sizes and their distance differs on n-Si and p-Si. During oscillations the Si electrodes are covered with an anodic oxide that has a mean thickness of about 10 nm, measured by *in-situ* FTIR on the asymmetric Si-O stretching mode and the integral oxide thickness varies periodically by 5 monolayers oxide coverage with the same frequency as the current but is phase shifted (see Fig.1).

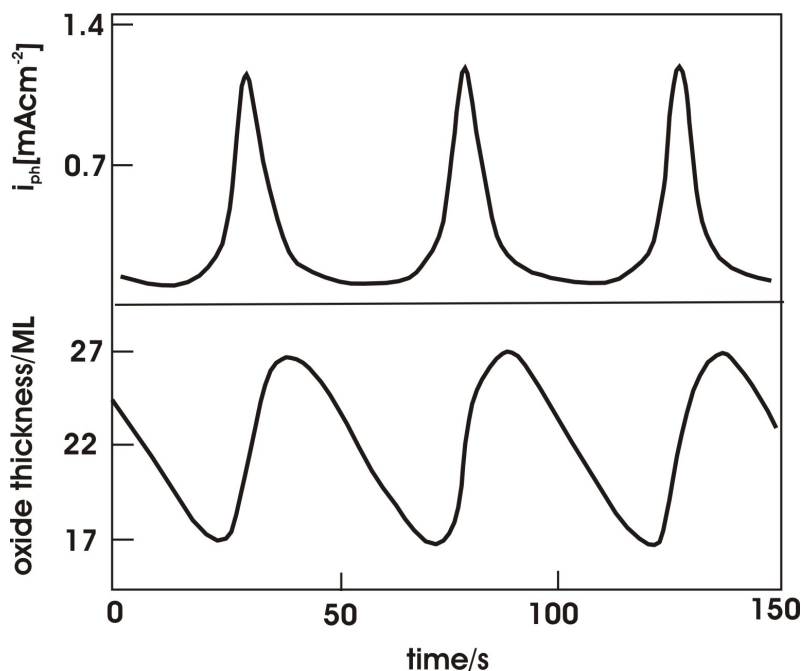


Fig.1: Oscillating behaviour of the photocurrent (top) and the oxide thickness (bottom), determined by *in-situ* FTIR; n-Si (111), electrode potential 6V (SCE); 0.1M  $\text{NH}_4\text{F}$ .

Fig.2 shows high resolution SEM images of nanopores formed during oscillatory behaviour on n-Si. Emersion of the sample was done at the increasing branch of the current, before the inflection point towards the current maximum. The pores that connect to the underlying silicon substrate allow for current flow that itself results in oxide growth. It has been found that pore morphologies, sizes and distance depends on the current phase at the time of sample emersion. The oscillatory behaviour has been described theoretically as a self-organized process where two types of oxides are formed which

show a substantially different etching behaviour. On a bare surface (which is present before our anodization procedure), initially formed oxides are supposed to grow rather undistortedly into the Si host whereas later formed oxide is more defecteous due to mismatch in the lattice parameters of Si and

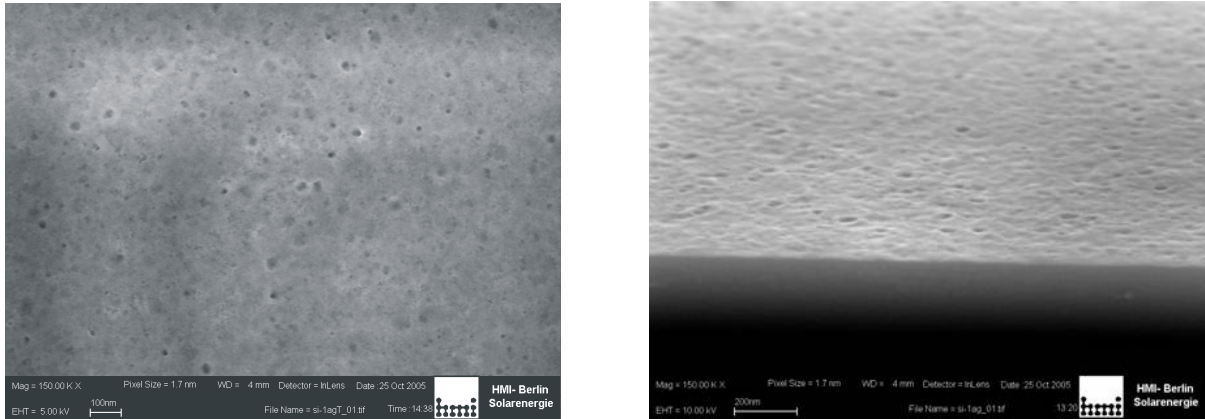


Fig.2: Top (left, scale 100 nm) and side (right, scale 200 nm) view HRSEM images of n-Si, oscillating for 200s at  $V = 6V$  (SCE) in  $0.1M NH_4F$ , pH 4 (see text).

its oxide. In the model [12,13], synchronization occurs in the etching period that is assumed to be longer than that for oxide growth. Accordingly, later formed oxides etch faster and the temporal

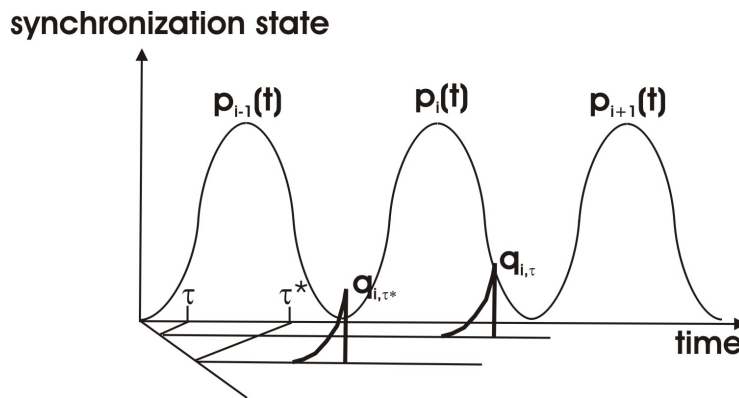


Fig.3: Schematic of the synchronization state  $p_i(t)$ , defined by markov-type integrals, and the contraction of the probability distribution of the cycle-time of the oscillating oxide thickness at an infinitesimal point on the Si surface (see text and refs.[12,13].

interval of the probability distribution of the cycle time for oxide thickness oscillators,  $q_{i,\tau^*}$ , contracts resulting in undamped functions  $p_i(t)$ , that describe the synchronization and are directly related to the current.

The nanopores, observed during current oscillations, can be used as templates for the construction of a solar cell where metallic nanoemitters operate as Schottky barrier metals: because of the insulating nature of the  $\sim 10$  nm thick oxide present during oscillations, spatially selective electrodeposition of metals into those pores that connect to the Si substrate becomes possible. Using Pt as a metal, for instance, such device can operate in the photovoltaic as well as the photoelectrolytic mode, generating hydrogen if p-Si is used as substrate. We show that selective deposition of metals into nanopores is possible and that solid state photovoltaic cells, photoelectrochemical light-to-electricity energy conversion and light-induced  $H_2$  evolution is possible. Initial devices are made at the Si/SiO<sub>2</sub>/Pt-nanocomposite/redox electrolyte contact and typical I-V characteristics for the photovoltaic mode are shown in Fig.4. Solar conversion efficiencies are in the range above 6 % for the early devices [14] where neither the oxide nor the various interfaces have been optimized. The results are obtained in a three-electrode potentiostatic arrangement, using Pt counter- and calomel reference electrode. Illumination is provided by W-I lamp where the spectral temperature is lower than that of the sun or

Xe high pressure lamps. The Wien shift results in a better spectral match to typical semiconductors than the sun, yielding a somewhat higher efficiency since less energy is lost by energetic photons.

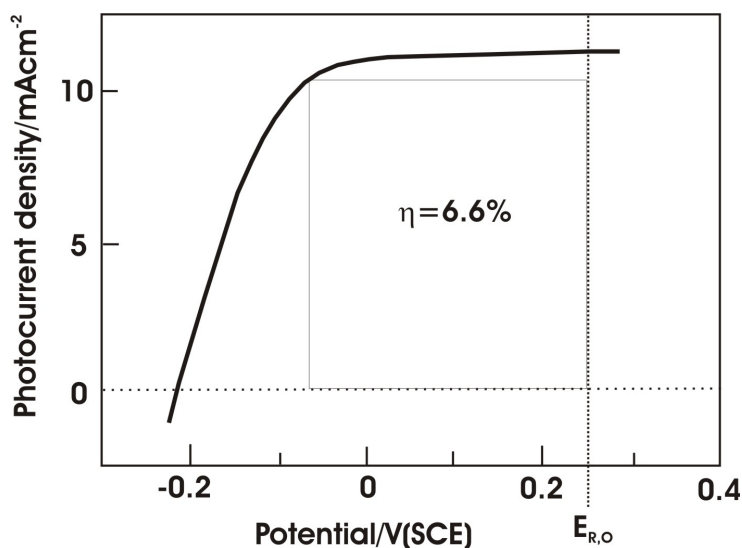


Fig.4: Photocurrent-voltage curves for n-Si/SiO<sub>2</sub>/Pt nanocomposite in I<sub>2</sub>/I<sup>-</sup> redox electrolyte illumination intensity: 50mWcm<sup>-2</sup>; fill factor 0.63; V<sub>OC</sub> 0.47V; i<sub>SC</sub> 2.72 mAcm<sup>-2</sup>.

### References

1. A. Uhler, Bell Syst. Tech. J., **35** (1956) 333
2. H.J. Lewerenz, M. Lübke, S. Menezes, K.J. Bachmann, Appl. Phys. Lett. **39** (1981) 798
3. M. Matsumura, S.R. Morrison, J. Electroanal. Chem. **144** (1983) 113
4. T. Bitzer, H.J. Lewerenz, Surf. Sci. **269/270** (1992) 886
5. H.J. Lewerenz, T. Bitzer, M. Gruyters, K. Jacobi, J. Electrochem. Soc. **140** (1993) L44
6. S. Rauscher, T. Dittrich, M. Aggour, J. Rappich, H. Flietner, H.J. Lewerenz, Appl. Phys. Lett. **66** (1995) 3018
7. H. Jungblut, J. Jakubowicz, S. Schweizer, H.J. Lewerenz, J. Electroanal. Chem. **527** (2002) 41
8. M. Lublow, H.J. Lewerenz, in preparation
9. O. Nast, S. Rauscher, H. Jungblut and H.J. Lewerenz, J. Electroanal. Chem. **422** (1998) 169
10. H.J. Lewerenz and M. Aggour, J. Electroanal. Chem. **351** (1993) 159
11. K. Skorupska, M. Aggour, M. Kanis, M. Lublow, H. Jungblut, H.J. Lewerenz, ECS Transactions **2** (2007) 63
12. J. Grzanna, H. Jungblut, H.J. Lewerenz, J. Electroanal. Chem. **486** (2000) 181; *ibid.* **486** (2000) 190
13. J. Grzanna, H. Jungblut, H.J. Lewerenz, AIP Conf. Proc. **780** (2005) 635
14. K. Skorupska, M. Aggour, T. Stempel-Pereira, M. Lublow, H.J. Lewerenz, Electrochem. Sol. State Lett., in press (2007)